Hindawi
Adsorption Science & Technology
Volume 2023, Article ID 6012467, 19 pages
https://doi.org/10.1155/2023/6012467

Research Article

Removal of Hexavalent Chromium by Using Sustainable Green Materials as Low-Cost Adsorbents

Qian Li,[1,2,3,4] **Qing Huang**,[1,2,3,4] **Fangqing Weng**,[1,2,3,4] **Wenqian Hu**,[1] **Jiamin Liu**,[1] **and Jiasheng Luo**[1]

[1]*Department of Chemistry and Life Science, Hubei University of Education, Wuhan 430205, China*
[2]*Hubei Environmental Purification Material Science and Engineering Technology Research Center, Hubei University of Education, Wuhan 430205, China*
[3]*Hubei Key Laboratory of Purification and Application of Plant Anti-Cancer Active Ingredients, Hubei University of Education, Wuhan 430205, China*
[4]*Hubei Engineering Technology Center of Environmental Purification Materials, Hubei University of Education, Wuhan 430205, China*

Correspondence should be addressed to Qian Li; liqian@hue.edu.cn

Received 6 June 2023; Revised 29 August 2023; Accepted 8 September 2023; Published 25 September 2023

Academic Editor: Adrián Bonilla-Petriciolet

The possibility of using three types of NaOH-treated tea residues (green tea, pu-erh, and tieguanyin) as low-cost adsorbents for Cr(VI) treatment was investigated. The surface charge, composition, morphology, structure, and functional groups in the obtained biosorbents were characterized by pH_{zpc}, cellulose content, SEM, BET, XRD, and FTIR spectroscopy. The nonlinear pseudo-first-order, pseudo-second-order, and Elovich models were used to investigate adsorption kinetics at various initial concentrations. The adsorption processes were more consistent with the pseudo-second-order kinetic model in the range of 5-50 mg L^{-1}. The adsorption isotherm at 298 K was described using the nonlinear Langmuir, Freundlich, Temkin-Pyzhev, and Dubinin-Radushkevich models, indicating that the process was favorable and complex with maximum adsorption amounts of 6.15, 19.50, and 12.31 mg g^{-1} for green tea, pu-erh, and tieguanyin residues, respectively. Thermodynamic analysis revealed that the adsorption was a spontaneous, endothermic process. The results demonstrated that all materials had the potential to successfully remove Cr(VI) from the aqueous solution.

1. Introduction

Heavy metal effluents discharged directly or illegally from the metallurgy, dye, electroplating, and textile industries are regarded as severe problems as a result of increasing modernization and industrialization. Depending on the types, sources, and concentrations of heavy metals, they can pose either short-term or long-term risks. Chromium is a typical heavy metal pollutant that has a bad effect on water bodies and human society. Even at low levels, chromium can harm the ecosystem and cause carcinogenic effects [1]. The most common chromium oxidation forms are Cr(VI) and Cr(III), the latter of which is a trace element required for life [2]. However, hexavalent chromium is the most harmful due to its higher oxidation state and diffusibility. Inhaling and holding Cr(VI)-containing materials can result in nasal septum perforation, asthma, bronchitis, pneumonia, laryngitis, liver inflammation, and a higher risk of bronchogenic carcinoma. Contact with Cr(VI) compounds can also cause skin allergies, dermatitis, and ulceration [3]. Many countries have been concerned for a long time about the detection and treatment of Cr(VI)-containing wastewater.

Over the years, many researchers have worked tirelessly to promote effective heavy metal removal methods such as membrane filtration, chemical precipitation, ion exchange, adsorption, electrocoagulation, and electrodialysis [4–6]. Adsorption, as one of the most promising techniques, has

the advantages of high selectivity, large adsorption capacity, and simple operation, which is favored by many scientists [7–9]. Recently, the use of diverse biomass materials as alternatives to high-cost adsorbents for the treatment of hazardous compounds has become a hot research issue [10–13].

Despite the benefits of adopting these locally accessible adsorbents, there are still difficulties in utilizing different treatment technologies. First, even though some materials are affordable, they may not be available in all nations with heavy metal contamination. Secondly, the normal adsorption capability of biosorbents is not sufficient due to the limited number of active sites. Some modifications are needed to increase the materials' ability to adsorb. Therefore, specialized knowledge and capabilities are required, which might not be appropriate for developing countries. Thus, to operate these adsorption systems, it is crucial to look for materials that are widely distributed and easy to use [14, 15].

Tea is one of the most commonly consumed beverages worldwide. Several researchers have reported that tea contains a variety of active groups and that the tea residue, a byproduct of tea consumption, also consists of various active ingredients, such as tea saponin, caffeine, purine bases, and amino acids, which may contribute to adsorption or complexation. Therefore, the utilization of tea residues has become one of the main focuses of the development of wastewater treatment technology. Recently, much published research has been carried out on the utilization of tea residue for the adsorption of various pollutants from wastewater [16–21]. China is the world's leading tea producer and consumer, with an annual production of 2.9 million tons in 2020 [22, 23]. Thus, there is a need to convert tea residues into useful adsorbents.

In this study, the three most common types of tea residues have been particularly chosen: green tea (nonfermented), pu-erh (post-fermented), and tieguanyin (semi-fermented), which were then simply treated with NaOH. This work is aimed at estimating the effect of the alkaline treatment on the properties of tea residues, comparing the adsorption capacity of different types of tea residues for the removal of Cr(VI) from wastewater samples, and determining the possible adsorption mechanism involved, therefore providing a possible sustainable technology to the problem of wastewater treatment and low-cost adsorbent development.

2. Methods

2.1. Preparation of Adsorbents. The three different types of tea residues (green tea, pu-erh, tieguanyin) used in the experiments were collected from a local market. To improve its adsorption capacity, the tea residues were mixed in a certain solid/liquid ratio (1 : 15, 1 : 20, 1 : 40, 1 : 50 w/v) with 1 mol L^{-1} NaOH at room temperature for 24 hours to ensure a complete reaction. The resulting mixture was then filtered, washed, and dried at 363 K for 10 hours. Finally, the materials were grounded and sieved to 200-400 μm for further use.

2.2. Adsorption of Cr(VI) on Modified Tea Residues. Adsorption tests were performed in a 100 mL beaker containing 50 mL of Cr(VI) solution at various initial concentrations. 0.2 g of adsorbent was added to the solution. The samples were then agitated in a magnetic stirrer at room temperature for 2 hours. The solution of 1 M HCl was used for pH adjustment. After centrifugation, the concentration of Cr(VI) in the supernatant was determined using a UV-visible spectrophotometer at $\lambda = 540$ nm. Finally, each adsorbent was rinsed with 50 mL of deionized water after adsorption and separated by centrifugation. The adsorption capacity q_t (mg g^{-1}) is calculated as follows:

$$q_t = \frac{(c_0 - c_t)}{m} \times V, \tag{1}$$

where c_0 (mg L^{-1}) and c_t (mg L^{-1}) are the Cr(VI) ion concentrations initially and at time t (min), m (g) is the mass of the tea residue, and V (L) is the volume of Cr(VI) solution.

Table 1: The mathematical equations of kinetic models.

Kinetic model	Nonlinear form
The pseudo-first-order kinetic model (PFO)	$q_t = q_e\left(1 - e^{-k_1 t}\right)$
The pseudo-second-order kinetic model (PSO)	$q_t = \frac{q_e^2 k_2 t}{1 + q_e k_2 t}$
The Elovich kinetic model	$q_t = \frac{1}{\beta} \ln(1 + \alpha\beta t)$

Table 2: The mathematical equations of isotherm models.

Isotherm model	Nonlinear form
The Langmuir isotherm	$q_e = \frac{q_m K_L c_e}{1 + K_L c_e}, q_e = \frac{q_m c_e}{b + c_e}$ $R_L = \frac{1}{1 + c_0/K_L}, R_L = \frac{1}{1 + bc_0}$
The Freundlich isotherm	$q_e = K_F c_e^{1/n}$
The Temkin-Pyzhev isotherm	$q_e = \frac{RT \ln Ac_e}{b_T}$
The Dubinin-Radushkevich isotherm	$q_e = q_m e^{-\beta\varepsilon^2}$ $\varepsilon = RT \ln\left(1 + \frac{1}{c_e}\right)$ $E = \frac{1}{(2\beta')^{1/2}}$

2.3. Adsorption Kinetics. In kinetic experiments, a 250 mL Cr(VI) solution with initial concentrations ranging from 5 to 50 mg L^{-1} was contacted with 1 g of tea residues at 298 K and a pH of 2. The supernatant was withdrawn at different time intervals and analyzed as before. Different kinetic models were applied to fit the kinetic data (Table 1).

q_e and q_t are the amounts of Cr(VI) adsorbed (mg g^{-1}) at equilibrium and at time t (min), respectively, k_1 (min^{-1}) and k_2 (g mg^{-1} min^{-1}) are the pseudo-first-order and pseudo-second-order rate constants, respectively, α is the initial adsorption rate (mg g^{-1} min^{-1}), and β is the desorption constant (g mg^{-1}).

2.4. Adsorption Isotherm. For the equilibrium studies, 1 g of tea residues was added to 250 mL of Cr(VI) solution at initial concentrations ranging from 5 to 50 mg L^{-1}. The

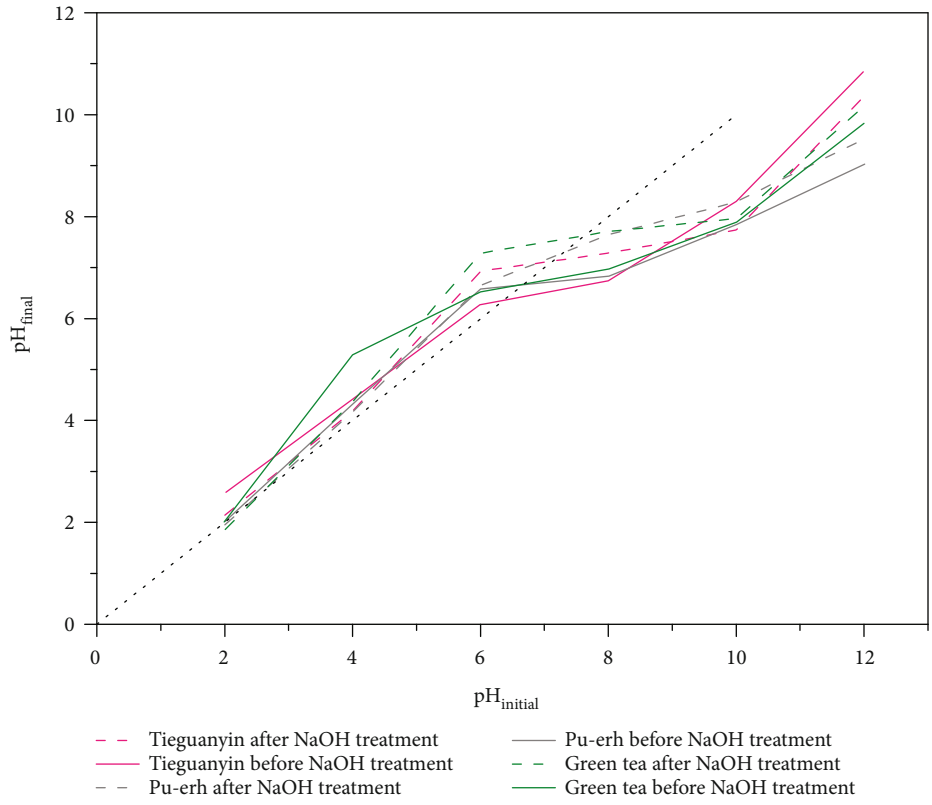

Figure 1: The pH_{zpc} of green tea, pu-erh, and tieguanyin before and after NaOH treatment.

Table 3: The content of cellulose in three types of tea residues (in wt%).

	Green tea	Pu-erh	Tieguanyin
Raw tea residue	8.60	12.27	18.72
NaOH-treated tea residue	15.61	27.34	32.30
Charge	+7.01	+15.07	+13.58

solution was agitated at different temperatures (298, 308, 323, 338, and 353 K) and a pH of 2 until equilibrium was reached (40 minutes for pu-erh, 180 minutes for tieguanyin, and 360 minutes for green tea). Four isotherm models (Langmuir, Freundlich, Temkin, and Dubunin-Radushkevich) were applied to describe the process (Table 2).

c_e is the equilibrium concentration of Cr(VI) (mg L^{-1}), q_m is the maximum adsorption capacity (mg g^{-1}), and K_L (mg L^{-1}) and b (L mg^{-1}) are the Langmuir constants. n is related to the intensity of adsorption, K_F (mg g^{-1} (mg $L^{-1})^{-1/n}$) is the Freundlich constant, b_T (J mol^{-1}) is the Temkin-Pyzhev isotherm constant related to the heat of adsorption, A (L g^{-1}) is Temkin-Pyzhev isotherm equilibrium binding constant, R (8.314 J mol^{-1} K^{-1}) is the universal gas constant, ε (J mol^{-1}) is the potential of Polanyi, β' (mol^2 kJ^{-2}) is the Dubinin-Radushkevich isotherm constant, T (K) is the absolute temperature, and E (kJ mol^{-1}) is the mean adsorption energy.

2.5. Characterization. The point of zero charge (pH_{zpc}) was determined using the following procedure [24]. 0.15 g of adsorbent was added to 50 mL of a 0.01 M NaCl solution and agitated with a magnetic stirrer. The pH was then adjusted to successive initial values between 2 and 12 by adding either HCl or NaOH. After 24 hours, the final pH of the solution was measured and plotted against the initial pH. The pH_{zpc} was calculated as the value where $pH_{final} = pH_{initial}$.

The amount of cellulose was measured using the method described by Liu et al. [25]. Briefly, 0.05-0.1 g of the desiccated sample was placed in a test tube. Then, 5 mL of the acetic and nitric acid mixture was added to the sample and heated in a boiling water bath for 25 minutes. The treated sample was filtered and washed several times with ionized water. After that, the sample was hydrolyzed with 10 mL of 72% H_2SO_4 and 10 mL of 0.01 mol L^{-1} K_2CrO_4 in a boiling water bath for 10 minutes. Finally, 5 mL of 20% KI and 1 mL of 0.5% $(C_6H_{10}O_5)_n$ were added and titrated with 0.02 mol L^{-1} $Na_2S_2O_3$. The amount of cellulose can be calculated as follows:

$$X = \frac{K(v_0 - v_1)}{(m \times 24)}, \quad (2)$$

where X is the amount of cellulose, K (mol L^{-1}) is the concentration of $Na_2S_2O_3$, v_0 (mL) is the amount of $Na_2S_2O_3$ consumed in blank samples, v_1 (mL) is the amount of $Na_2S_2O_3$ consumed in samples, and 24 is the equivalent number of 1 mol $(C_6H_{10}O_5)_n$ to $Na_2S_2O_3$.

The morphology was studied using scanning electron microscopy (SEM, FEI Quanta 200, USA). XRD

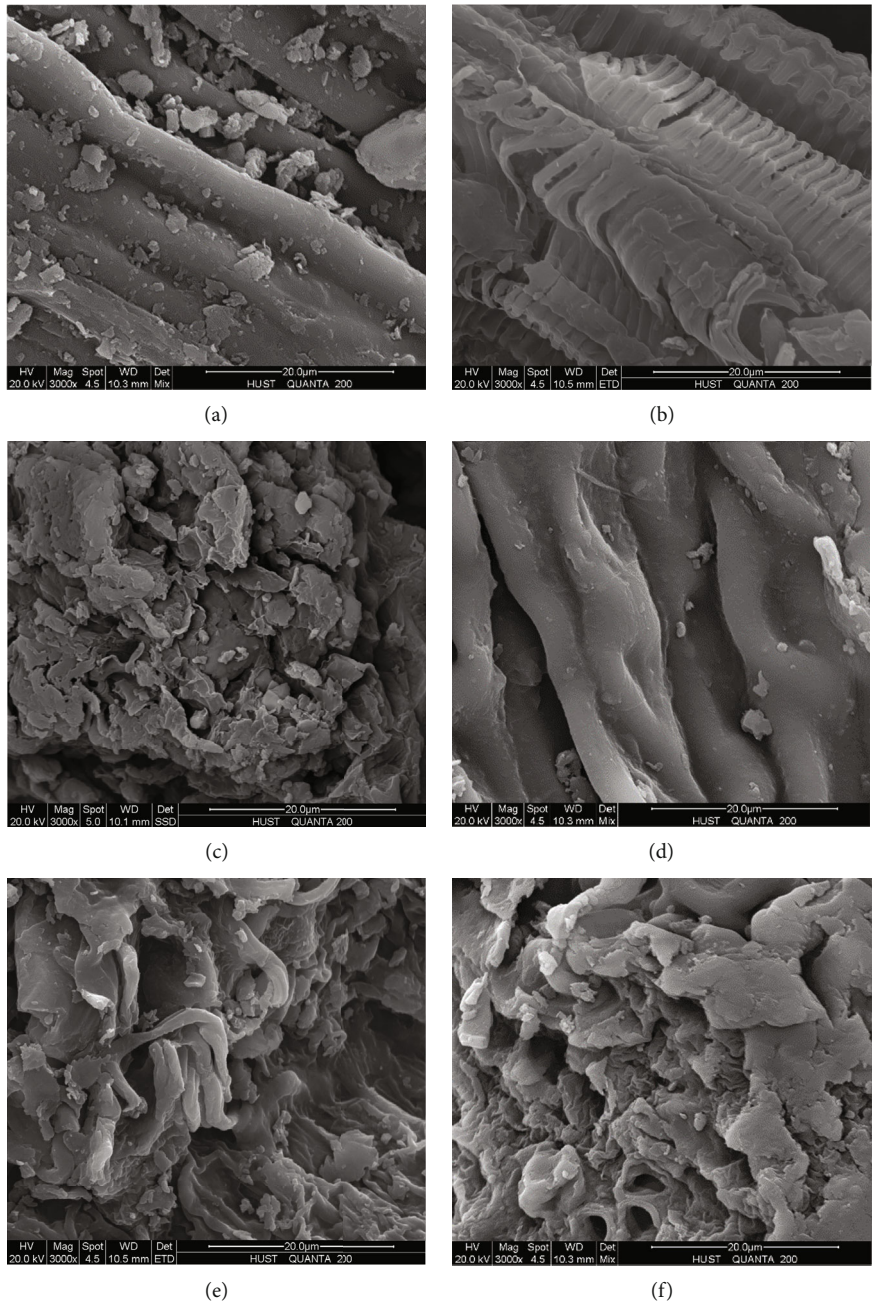

Figure 2: SEM images of (a) green tea, (b) pu-erh, and (c) tieguanyin before NaOH treatment; (d) green tea, (e) pu-erh, and (f) tieguanyin after NaOH treatment.

measurements were carried out on the powder X-ray diffractometer (Bruker Phaser-D2, German). The surface functional groups of adsorbents were measured by FT-IR spectra (Nexus ThermoNicolet, USA) using KBr pellets. The surface area and pore volume were measured in a BET surface area analyzer (BSD-PM2-1203, China) at liquid nitrogen temperature (77 K).

2.6. Statistical Analysis. The Origin 7.5 software (Origin Lab, version 7.5, USA) was used to analyze and graph the experimental data.

3. Results and Discussion

3.1. Determination of pH_{zpc}. The pH_{zpc} is an important parameter in adsorption processes because it identifies the pH value at which the charges at the adsorbent's surface shift from anionic ($>pH_{zpc}$) to cationic ($<pH_{zpc}$) [26]. Adsorption of cations is favored at pH values greater than pH_{zpc}, whereas that of anions is favored at pH values less than pH_{zpc}.

As shown in Figure 1, the values of pH_{zpc} obtained before and after NaOH treatment were 6.6 and 7.6 for green

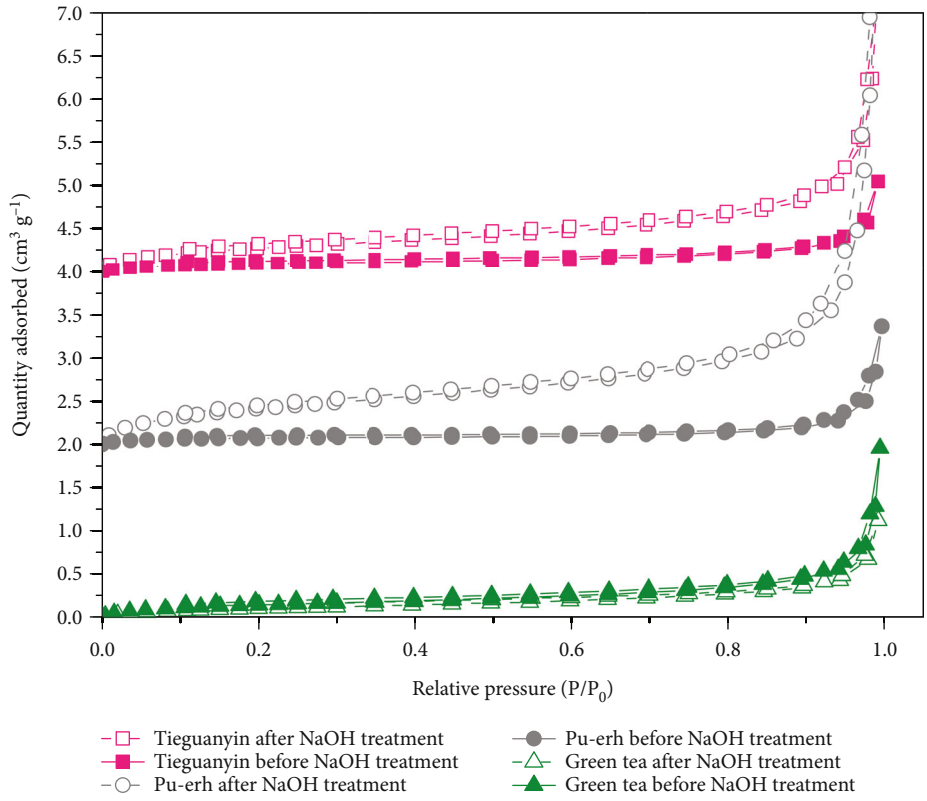

Figure 3: Nitrogen adsorption/desorption isotherms at 77 K of the green tea, pu-erh, and tieguanyin.

Table 4: The BET results of three types of tea residues before and after NaOH treatment.

	Green tea	NaOH-treated green tea	Pu-erh	NaOH-treated pu-erh	Tieguanyin	NaOH-treated tieguanyin
BET surface area (m^2 g^{-1})	0.56	0.41	0.28	1.61	0.36	1.08
The average pore diameter (nm)	14.65	11.53	23.90	17.75	15.45	14.11

tea, 6.6 and 7.2 for pu-erh, and 6.3 and 7.1 for tieguanyin. This increase in pH_{zpc} values suggested the adsorbent surfaces were more positively charged at the experimental pH, which in turn increased the Cr(VI) anions' adsorption attraction. These results were consistent with recent research by Anjum et al. [27], Azzaz et al. [28], Zhao and Dai [29], and Patel et al. [30].

3.2. Content of Cellulose. Table 3 shows the content of cellulose in three types of tea residues. Before NaOH treatment, the cellulose content of the green tea, pu-erh, and tieguanyin residues was 8.60%, 12.27%, and 18.72%, respectively. Significantly higher cellulose content was obtained for the samples of NaOH-treated green tea (34.91%), pu-erh residues (27.34%), and tieguanyin (32.3%), indicating that alkaline treatment facilitated the removal of hemicelluloses, pectin, and lignin, which agreed with the previous results [31].

3.3. SEM Analysis. Figure 2 represents the SEM images of three types of tea residues before and after NaOH treatment. In Figure 2(a), it was clearly shown that the surface of untreated green tea residue was irregular, rough, and covered with impurities like hemicellulose, lignin, and waxy elements. These impurities generally cover the cellulosic hydroxyl groups, preventing them from interacting with the adsorbate. After treatment with alkaline, the green tea residue changed significantly (Figure 2(d)), becoming cleaner and smoother as the noncellulosic components were removed from the surface. The untreated pu-erh residue flocculated into a group with many loops and humps (Figure 2(b)). The NaOH caused the fiber to begin to crack into small pieces during alkaline treatment, which resulted in an increase in surface area (Figure 2(e)). In the case of tieguanyin residue, it exhibited a compact structure that might result from hydrogen bonding, covalent O-H bonds, and Van der Waal interactions between cellulose, hemicellulose, and lignin (Figure 2(c)). The noncellulosic complexes were partially removed after alkaline treatment, exposing more porosity and surface area of the cellulose that had previously been hidden (Figure 2(f)). According to the findings, pretreatments of three types of tea residues with alkaline treatment using NaOH helped to open the cellulosic fiber and improve surface functionality, making them more accessible for interaction with Cr(VI) and enhancing adsorption

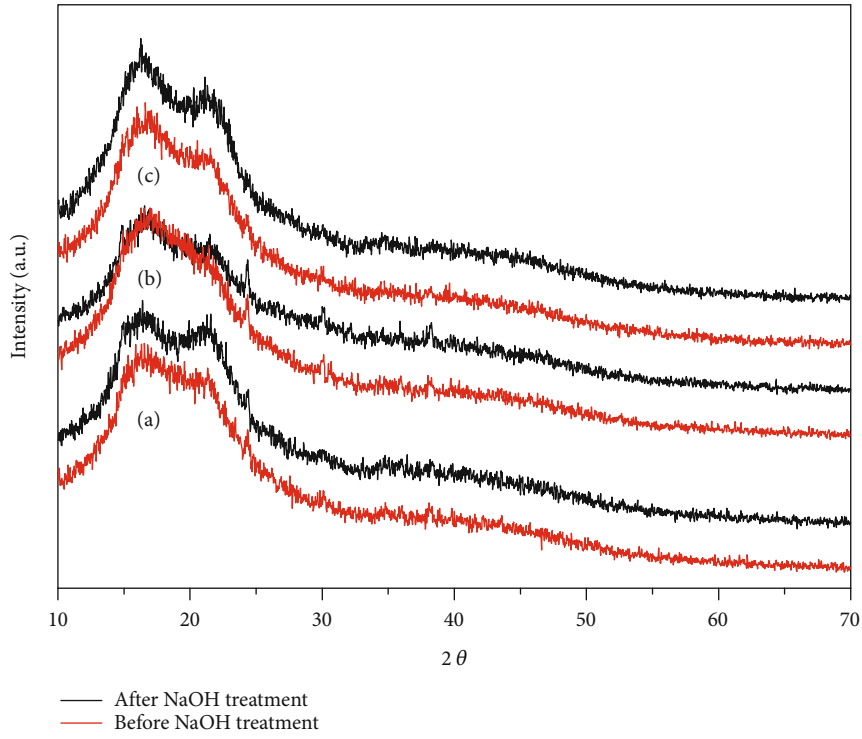

Figure 4: XRD patterns of (a) green tea, (b) pu-erh, and (c) tieguanyin before and after NaOH treatment.

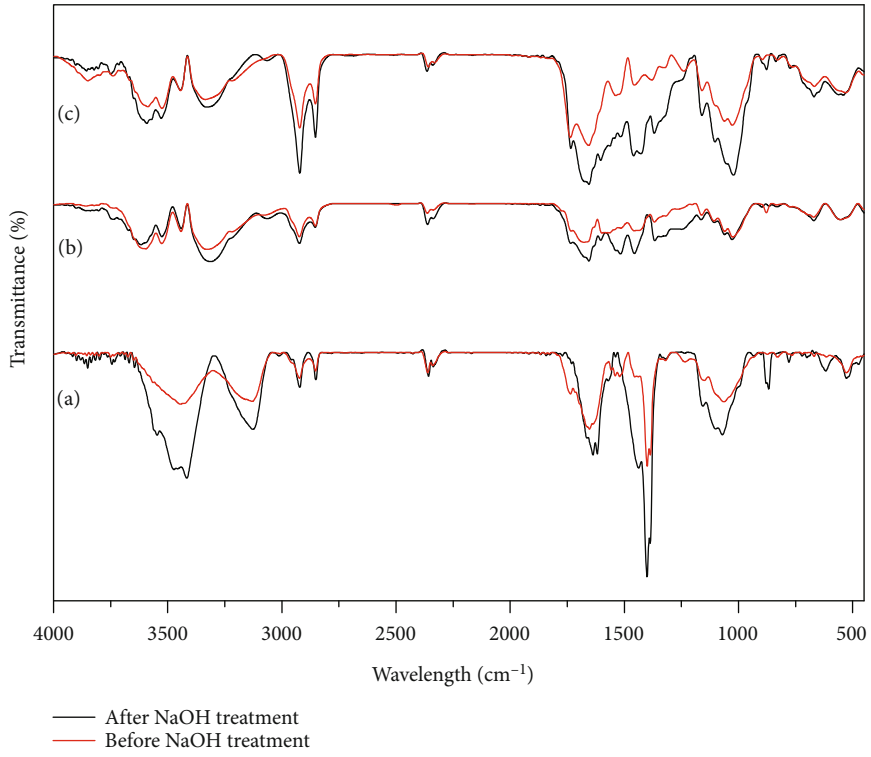

Figure 5: FTIR spectra of (a) green tea, (b) pu-erh, and (c) tieguanyin before and after NaOH treatment.

capacity. The alkaline treatment promoted the dissolution of noncellulosic constituents and changed the structure and morphology of tea residues. Similar results have also been reported in previous studies [32–35].

3.4. BET Analysis. The impact of NaOH treatments on the surface characteristics of the tea residues was further confirmed by the nitrogen adsorption analysis. Figure 3 displays the N_2 adsorption and desorption isotherms of both original

Table 5: The surface functional group shift in peaks.

	Wave number range (cm^{-1}) before treatment	Wave number range (cm^{-1}) after treatment	Assignment
Green tea residue	3444	3416	-OH or N-H
	3130	3128	-OH or N-H
	2923	2923	Aliphatic C-H
	2852	—	Aliphatic C-H
	1736	—	C=O
	1653	1637	C=O
	1400	1401	Phenyl groups
	1386	—	Aliphatic C-H group
	1235	—	$-SO_3$ stretching/P=O, C-O
	1150	—	C-O-C
	1064	1071	C-O
Pu-erh residue	3441	3441	-OH or N-H
	3312	3328	-OH or N-H
	3063	—	-OH or N-H
	2923	2923	Aliphatic C-H
	2854	—	Aliphatic C-H
	1655	1678	C=O
	1517	—	Amide II of proteins, N-H, C-N
	1456	1456	N-H bending, C-H
	1367	—	Aliphatic C-H group
	1106	—	C-O-C
	1028	1025	C-O
Tieguanyin residue	3443	—	-OH or N-H
	3335	3330	-OH or N-H
	2922	2922	Aliphatic C-H
	2853	2853	Aliphatic C-H
	1736	—	C=O
	1656	1655	C=O
	1537	—	Amide II of proteins, N-H, C-N
	1456	1459	N-H bending或C-H
	1380	—	Aliphatic C-H group
	1240	—	$-SO_3$ stretching/P=O, C-O
	1160	—	C-O-C
	1067	1022	C-O

and modified tea residues. All three types of tea residues exhibited a type IV isotherm, suggesting the characteristics of nonporous and macroporous adsorbents. The desorption process showed a minor hysteresis, which could be attributed to the amorphous phase that generated macropores at the exterior surface [36].

Based on N_2 adsorption and desorption analysis, the specific surface areas and average pore diameters were calculated. Table 4 shows that after alkali treatment, pu-erh and tieguanyin tea residues greatly increased in specific surface area and average pore diameter. The specific surface of pu-erh and tieguanyin tea residues was 5.75 and 3 times that before modification, respectively. The average pore diameter decreased by 21.3%, 25.73%, and 8.67% for green tea, pu-erh, and tieguanyin tea residues, respectively. The cracks and holes in the treated tea residues' outer and cross-sectional surfaces had an effect on surface areas. NaOH treatment resulted in the formation of mesopores. This outcome matched the findings of an earlier SEM analysis of the study's sample materials. While NaOH treatment increased the surface areas of pu-erh and tieguanyin residues, it had the reverse effect on green tea residue, which might be a result of the partial framework collapsing. As a result, the surface area of treated green tea was not increased following NaOH treatment [37, 38].

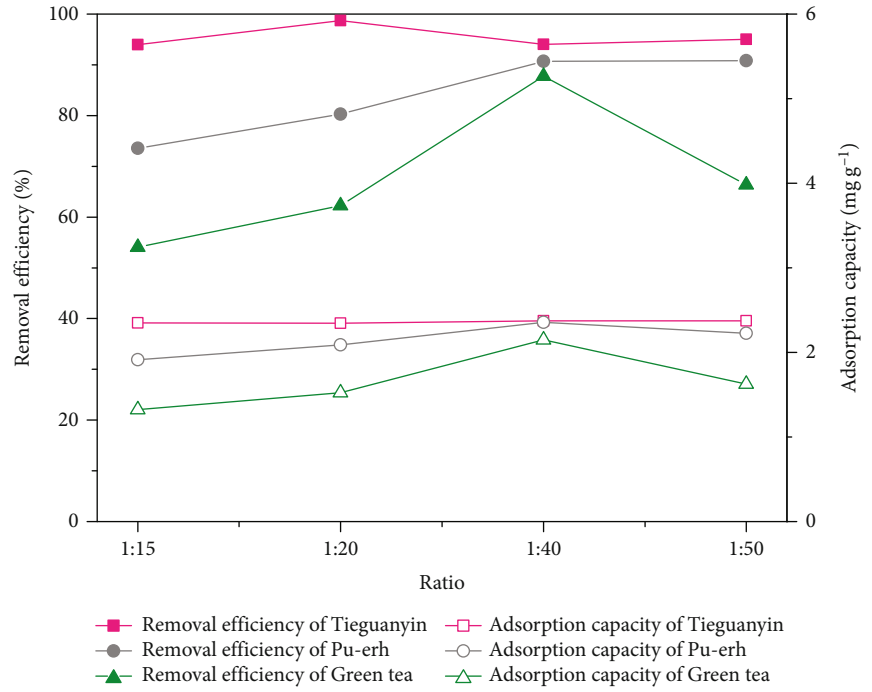

Figure 6: The effect of tea residues: NaOH (S/L) ratio on Cr(VI) adsorption onto tea residues.

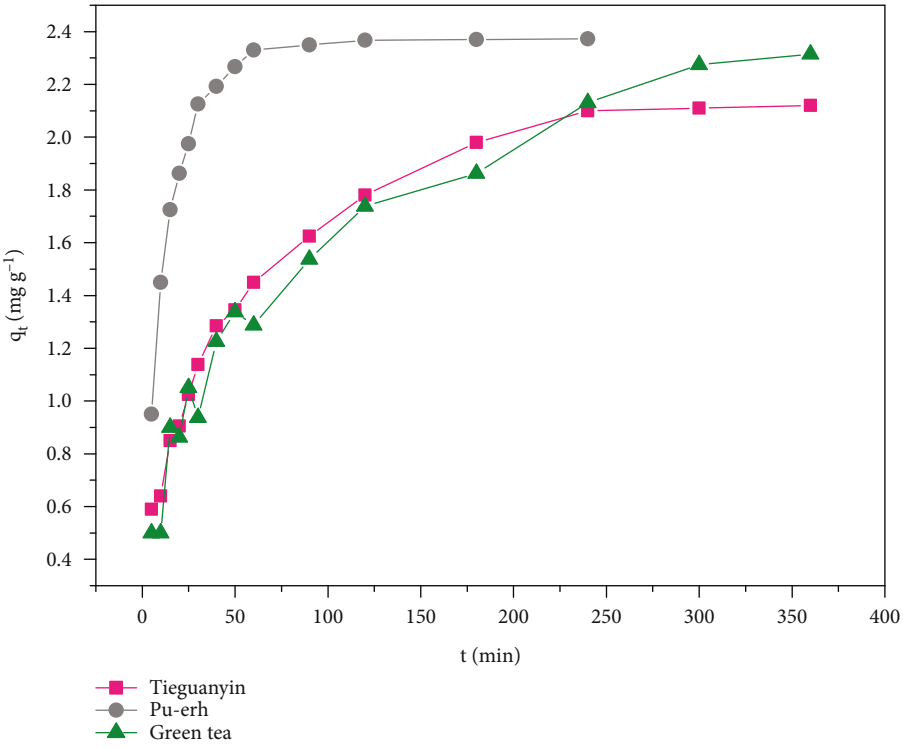

Figure 7: Kinetic curves for Cr(VI) adsorption onto tea residues.

3.5. XRD Analysis. Further studies were performed in order to better understand the impact of the alkaline treatment on the crystalline structure of the tea residues. The phase and crystallinity of the untreated and NaOH-treated samples were evaluated using X-ray diffraction (XRD). Typical diffraction patterns are shown in Figure 4.

As seen in Figure 4, the XRD patterns of the raw and modified tea samples showed significant amorphous regions. Two broader peaks at 16.54° and 20.46° for green tea, 16.3° and 19.2° for pu-erh, and 15.98° and 19.7° for tieguanyin appeared in the untreated tea residues, respectively. These peaks correlated with the cellulose I structure and are

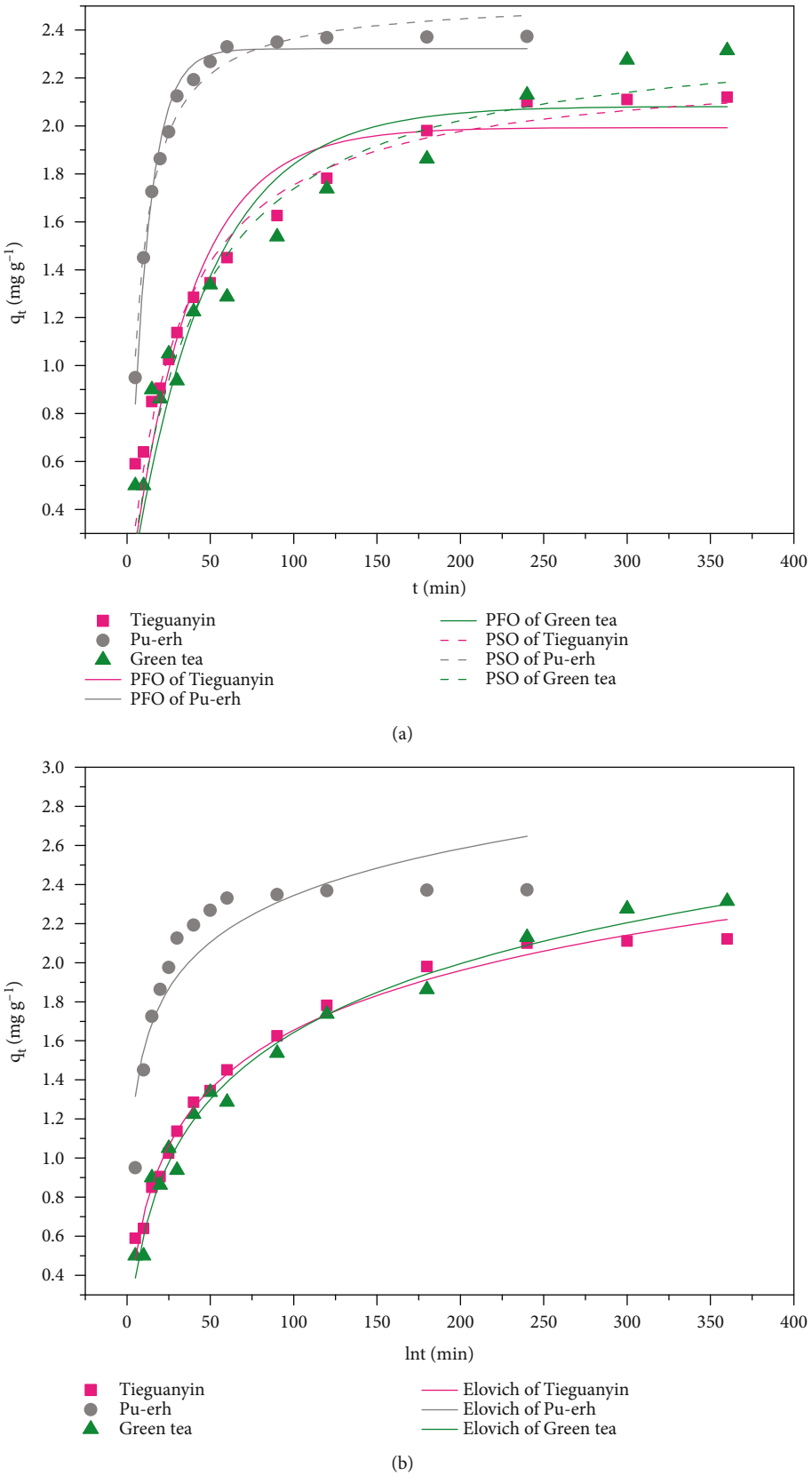

Figure 8: Adsorption kinetics for Cr(VI) adsorption onto tea residues: (a) pseudo-first-order and pseudo-second-order kinetic model and (b) Elovich kinetic model.

Table 6: Parameters of pseudo-first-order, pseudo-second-order, and Elovich models for Cr(VI) adsorption onto tea residues at different initial concentrations.

	Green tea residue	Pu-erh residue	Tieguanyin residue
$q_{e,\exp}$ (mg g^{-1})	2.32	2.37	2.1
Pseudo-first-order			
$q_{e,\mathrm{cal},1}$ (mg g^{-1})	2.08	2.32	1.99
k_1 (min^{-1})	2.16×10^{-2}	8.99×10^{-2}	2.72×10^{-2}
R^2	0.8948	0.9787	0.9203
Pseudo-second-order			
$q_{e,\mathrm{cal},2}$ (mg g^{-1})	2.42	2.53	2.26
k_2 (g mg^{-1} min^{-1})	1.05×10^{-2}	5.49×10^{-2}	1.52×10^{-2}
R^2	0.9511	0.9836	0.9727
Elovich			
α (mg g^{-1} min^{-1})	0.11	3.03	0.17
β (g mg^{-1})	1.90	2.89	2.22
R^2	0.9815	0.8271	0.9888

consistent with the high levels of lignin and hemicellulose that contributed to the amorphous phase [35].

The XRD patterns after modification demonstrated that alkali treatment not only noticeably affected the position, shape, and intensity of the main peaks in treated samples but also caused some peaks to become slightly more defined. Some corresponding peaks shifted to the $2\theta = 21.28°$, 21.52°, and 21.8° for green tea, pu-erh, and tieguanyin, respectively. These distinct peaks might indicate the transition of cellulose I into cellulose II [39].

Additionally, the characteristic diffraction peaks of green tea and pu-erh gradually weakened. The peaks of the alkali-treated tieguanyin residue, however, were sharper and larger than those of the untreated samples, indicating that the amorphous regions were largely destroyed following the alkaline treatment, which also resulted in an increase in crystallinity [40]. This conclusion was in line with the earlier cellulose examination of samples used in the study.

3.6. FTIR Analysis. FTIR analysis was performed to evaluate the characteristics of functional groups in the tea residues before and after alkali treatment. Figure 5 shows a comparison between FTIR spectra obtained for raw tea residues and NaOH-treated samples. Typically, the broad, strong peaks at 3440-3063 cm^{-1} indicated the existence of surface hydroxyl groups (-OH). The peaks at 2922-2852 cm^{-1} corresponded to the aliphatic C-H group [41]. The peaks at 1736-1653 and 1656-1653 cm^{-1} were assigned to C=O stretching and N-H bending, which were the bonds of hemicellulose, lignin, and amino acids. The peaks located at 1537-1517 cm^{-1} indicated the secondary amine group [42]. The peaks that appeared at 1456, 1400, and 1386-1367 cm^{-1} were attributed to N-H bending, phenyl groups, and -CH_3 bending. Besides, the peaks at 1240-1235, 1160-1106, and 1028-1067 cm^{-1} were related to -SO_3 stretching, C-O-C groups, and C=O groups, respectively. Overall, the tea residues, which consisted of cellulose, hemicellulose, and lignin components, were confirmed by the existence of alkanes, esters, aromatics, ketones, amines, and alcohols [43].

In contrast, it was clear that the NaOH-treated tea residues showed some changes compared to the spectra of the raw tea residues. As shown in Figure 5, the carbonyl groups (C=O) and hydroxyl groups (-OH) increased significantly in all NaOH-treated samples, indicating a high ionic exchange capacity to uptake Cr(VI) from the solution. In addition, the fact that treating tea residues with NaOH changed the surface functional group was also evident by the shift in peaks shown in Table 5. Furthermore, the absorption bands of the aliphatic C-H groups, C=O stretching, C-O-C groups, and the secondary amine group were not detected when compared to those cellulose samples due to the hydrolysis of carbonyl groups and the elimination of noncellulosic constituents in alkaline solutions [44].

3.7. The Effect of Tea Residues: NaOH (S/L) Ratio on Cr(VI) Adsorption. The effect of NaOH modification on adsorbent adsorption performance was also investigated (Figure 6). In all three cases, the presence of NaOH initially increased the adsorption capacity and removal efficiency of Cr(VI). At a 1 : 40 ratio, green tea (87.76%, 2.15 mg g^{-1}) and pu-erh (90.67%, 2.36 mg g^{-1}) showed the highest removal efficiency and adsorption capacity. However, the highest removal efficiency (98.72%) and adsorption capacity (2.34 mg g^{-1}) of tieguanyin residue were observed at a ratio of 1 : 20.

It is worth noting that the removal efficiencies of Cr(VI) for NaOH-treated tea residues were higher than for raw tea residues. This was explained by the fact that the alkali treatment altered the chemical composition of the tea by producing more O-Na sites that could bond with Cr(VI) molecules. Similar results have been observed in other research [28].

3.8. Adsorption Kinetics. Figure 7 depicts the change in the adsorption capacity versus the contact time for three different types of tea residues with an adsorbent dosage of 1 g

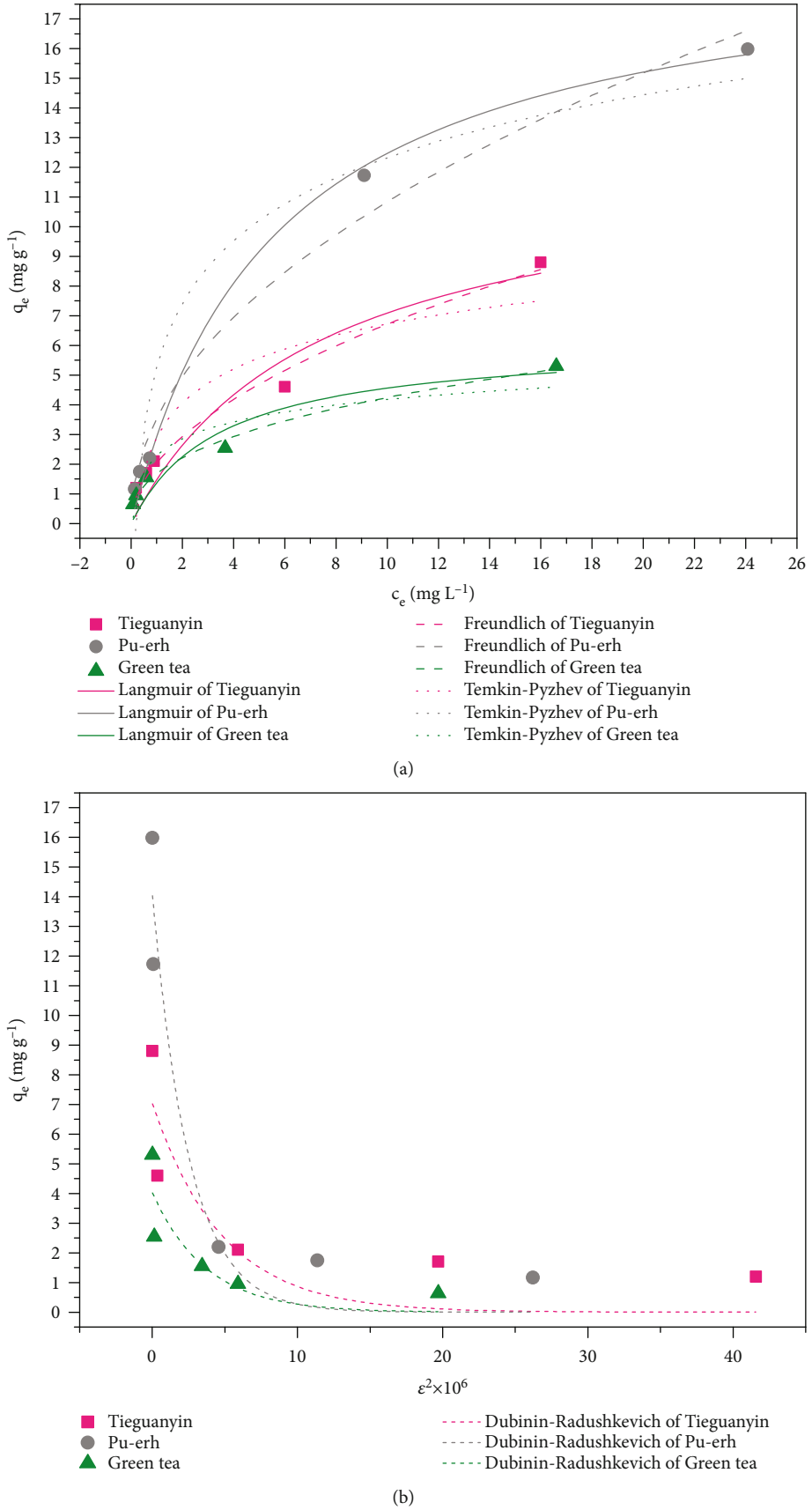

Figure 9: Adsorption isotherms for Cr(VI) adsorption onto tea residues at 298 K: (a) Langmuir adsorption isotherm, Freundlich adsorption isotherm, and Temkin-Pyzhev adsorption isotherm and (b) Dubinin-Radushkevich adsorption isotherm.

Table 7: Parameters of different isotherms at 298 K.

	Green tea residue	Pu-erh residue	Tieguanyin residue
Langmuir			
q_m (mg g^{-1})	6.15	19.50	12.31
b (L mg^{-1})	0.29	0.18	0.14
R_L	0.07-0.41	0.10-0.53	0.13-0.6
R^2	0.8954	0.9949	0.9260
Freundlich			
K_F (mg g^{-1} (mg L^{-1})$^{-1/n}$)	1.67	3.54	2.04
n	2.48	2.06	1.94
R^2	0.9903	0.9830	0.9872
Temkin-Pyzhev			
b_T (kJ mol^{-1})	3.01	0.81	1.49
A (L g^{-1})	16.06	5.66	5.76
R^2	0.8976	0.9530	0.8797
Dubinin-Radushkevich			
E (kJ mol^{-1})	1.36	1.13	1.54
q_m (mg g^{-1})	4.04	14.09	7.06
R^2	0.7271	0.9378	0.7246

and a 250 mL Cr(VI) solution of 10 mg L^{-1} at 298 K. The adsorption capacity for each tea residues increased rapidly in the first 100 minutes and tended to level off afterward. It is worthy of note that both green tea and tieguanyin residues had comparable adsorption kinetics, whereas the adsorption of pu-erh was faster initially, and the contact time required for adsorption equilibrium was much shorter for pu-erh residue than that for green tea and tieguanyin residues. In addition, the q_t values of pu-erh were consistently higher than those of green tea and tieguanyin at every time interval, demonstrating that it was the best adsorbent for Cr(VI).

This can be explained by the fact that, initially, the active sites on the tea residues surface would be occupied due to the complexation of the -OH and C=O groups with the metal ions; the adsorption was predominated by chemisorption, whereas at later times, the adsorption developed slowly, possibly indicating adsorption by diffusion. However, these processes are also governed by particle size and the point of zero charge.

The nonlinear pseudo-first-order, pseudo-second-order, and Elovich models were used to fit the experimental data for three types of tea residues (Figure 8), and the results obtained are shown in Table 6. It can be inferred from Table 6 that the pseudo-second-order kinetic model fitted the kinetic data better than the other two models for three types of tea residues, with R^2 values greater than 0.95. Moreover, the calculated equilibrium adsorption amount $q_{e,\mathrm{cal},2}$ was comparable to the experimental values $q_{e,\mathrm{exp}}$. The kinetic rate constant k_2 for pu-erh (5.49×10^{-2} g mg^{-1} min^{-1}) was greater than for green tea (1.05×10^{-2} g mg^{-1} min^{-1}) and tieguanyin (1.52×10^{-2} g mg^{-1} min^{-1}), which agreed with the experimental results. In conclusion, the pseudo-second-order model was better suited for predicting Cr(VI) adsorption onto three different types of tea residues, indicating the role of chemical adsorption in this process [7, 45].

The Elovich model was also used to look into the chemisorption hypothesis for the heterogeneous system in more detail. It turned out that the Elovich model was discovered to be the most suitable for green tea and tieguanyin, indicating that these adsorption processes may occur on heterogeneous surfaces and that chemisorption may be involved in Cr(VI) adsorption onto these two tea residue surfaces [46]. Some carbonate groups that were present on the shell surface may have played a role in forming bonds with the Cr(VI) ion molecules. The outcome and the FTIR analysis results were in good agreement.

3.9. Adsorption Isotherms. To further analyze the interaction between Cr(VI) and tea residues, the equilibrium adsorption data for different initial concentrations at 298 K were analyzed using different isothermal adsorption models, and the fitting results are shown in Figure 9 and Table 7.

It was observed that the Langmuir model provided a good description of the interaction between pu-erh residue and Cr(VI) in terms of the values of $R^2 > 0.99$. The maximum adsorption amounts calculated from this model were 6.15, 19.50, and 12.31 mg g^{-1} for green tea, pu-erh, and tieguanyin, respectively, revealing that pu-erh had the highest adsorption capacity. And the values R_L in all cases were between 0 and 1, indicating a favorable process and a strong relationship between the tea residues and Cr(VI) [47].

As compared to other models, the Freundlich model showed the best degree of fit, as indicated by values of R^2 of 0.9903, 0.9830, and 0.9872 for green tea, pu-erh, and tieguanyin, respectively. Similar conclusions have been recorded previously [48–51]. The distribution of pore sizes

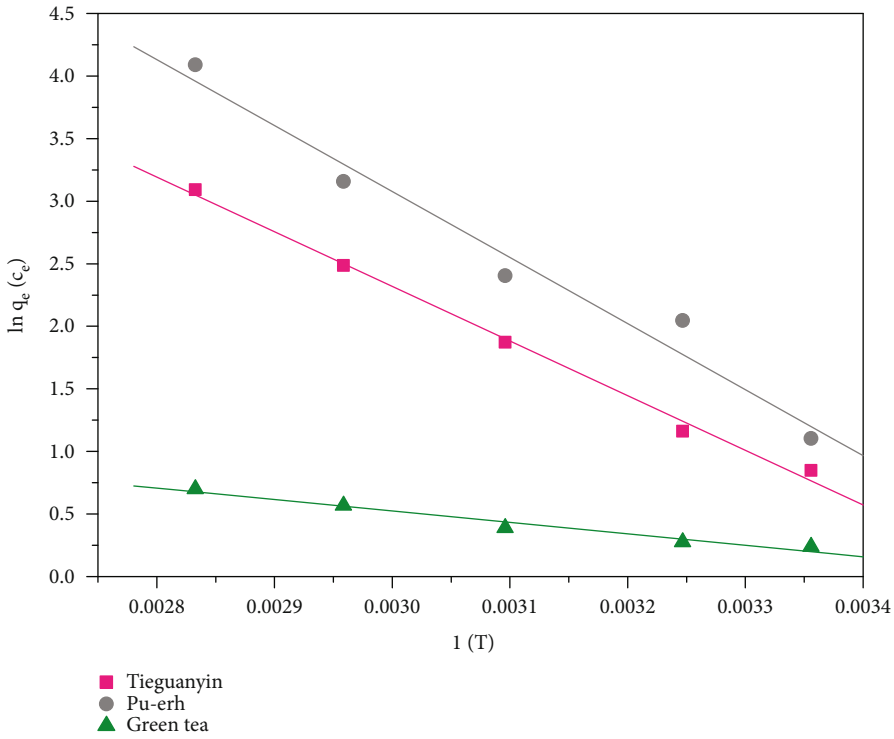

Figure 10: Thermodynamics for Cr(VI) adsorption onto tea residues.

Table 8: Thermodynamic parameters for Cr(VI) adsorption onto tea residues.

Adsorbents	$\Delta H^{\ominus}$ (kJ mol^{-1})	$\Delta S^{\ominus}$ (J mol^{-1} K^{-1})	$\Delta G^{\ominus}$ (kJ mol^{-1})				
			298 K	308 K	323 K	338 K	353 K
Green tea residue	7.62	27.22	-0.49	-0.76	-1.17	-1.58	-1.99
Pu-erh residue	4.39	157.17	-2.97	-4.55	-6.9	-9.26	-11.62
Tieguanyin residue	36.3	128.19	-1.9	-3.18	-5.1	-7.03	-8.95

and the presence of functional groups on the surfaces of the tea residues contributed significantly to their high degree of heterogeneity. The heterogeneous nature is also consistent with the results of the Elovich kinetic analysis. Additionally, the heterogeneity parameter n indicates the favorability of adsorption. If n is between 1 and 10, the adsorption is favorable. Table 7 shows that the values of n in all three cases were greater than one, indicating that the adsorption of Cr(VI) onto the three types of tea residues was favorable [10, 17].

The average adsorption energy E calculated from the Dubinin-Radushkevich isotherm model was less than 8 kJ mol^{-1}, implying that physical adsorption took place at 298 K [28, 52, 53]. Thus, the adsorption of Cr(VI) onto pu-erh was a complex process that involved physical and chemical adsorption, as well as monolayer and multilayer adsorption. But owing to the low values of R^2, this model might not adequately describe the adsorption processes of green tea and tieguanyin.

For the Temkin-Pyzhev isotherm model, the R^2 values were greater than 0.95 for the pu-erh residue, indicating that electrostatic interaction was an important mechanism during the adsorption process. The magnitude of b_t (adsorption heat) indicated that the adsorption process was feasible with high Cr(VI) coverage on the surface of biosorbents, and this type of tea residue had strong chromium affinities. Similar results have been reported before [54, 55]. However, for the green tea and tieguanyin, the Temkin fittings appeared to deviate from the experimental data.

In general, among the four studied isotherms, the Freundlich isotherm provided the greatest match to the experimental results, as shown in Table 7. The findings suggested that the adsorption of Cr(VI) onto the three tea residues might occur on the heterogeneous active sites present on the adsorbent surfaces.

3.10. Adsorption Thermodynamics. The following equations can be used to calculate the thermodynamic parameters of chromium adsorption by tea residues:

$$\begin{aligned} \Delta G^{\ominus} &= \Delta H^{\ominus} - T\Delta S^{\ominus}, \\ \Delta G^{\ominus} &= -RT \ln K_e = -RT \ln \frac{q_e}{c_e}, \\ \ln \frac{q_e}{c_e} &= -\frac{\Delta H^{\ominus}}{RT} + \frac{\Delta S^{\ominus}}{R}, \end{aligned} \tag{3}$$

where K_e is the distribution coefficient of the adsorbate.

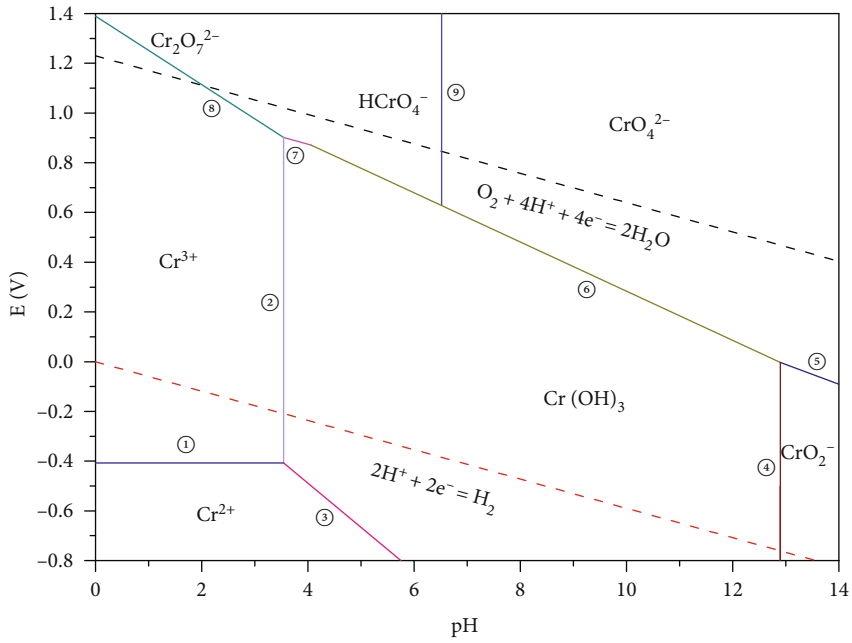

Figure 11: Distribution of Cr(VI) species.

Using the experimental data at 298-353 K, the $\Delta H^{\ominus}$ and $\Delta S^{\ominus}$ were calculated from the slope and intercept by plotting $\ln q_e/c_e$ against $1/T$, and the $\Delta G^{\ominus}$ was estimated at different temperatures. The results obtained are shown in Figure 10 and Table 8.

As can be seen from Table 8, the positive values of $\Delta H^{\ominus}$ for each tea residues suggested that the adsorption processes were endothermic. Moreover, when the $\Delta H^{\ominus}$ value is between -40 and -600 kJ mol^{-1}, the adsorption process is generally driven chemically. Accordingly, the experimental results revealed that in the case of green tea, in the present experimental range, chromium adsorption might involve physical adsorption due to electrostatic attraction, hydrogen bonding, and ligand group exchange. As for pu-erh and tieguanyin residues, the process might involve chemical adsorption, which confirmed the previous analysis.

At different temperatures, $\Delta G^{\ominus}$ values for the three types of adsorbents were negative, suggesting the spontaneity nature of the adsorption of Cr(VI) onto green tea, pu-erh, and tieguanyin residues. And they became more negative with increasing temperature, meaning the adsorption is more favorable at higher temperatures. This result was consistent with other reports obtained by Villabona Ortíz et al. (2020) [56]. Furthermore, the fact that the absolute values of $\Delta G^{\ominus}$ were less than 40 kJ mol^{-1} showed that the adsorption in this study appeared to be a physicochemical sorption process instead of a simple physical or chemical adsorption process [57].

The increase in disorder at the solid-liquid interface during the adsorption process was reflected in the positive values of $\Delta S^{\ominus}$, indicating a high affinity of Cr(VI) for the adsorbents [58, 59]. This endothermic and disordered nature of tea residue-chromium adsorption could be due to a possible hexavalent chromium reduction reaction as well as physical adsorption in this adsorption process, which was consistent with previous research [60, 61].

3.11. Possible Adsorption Mechanism. According to FTIR research, the three types of tea residues were found to contain C=O bonds, carboxylic acids, amines, phenolics, and amide groups, all of which have been shown to be highly effective at removing Cr(VI) ions from wastewater. The existence of C=O bonds can create hydrogen bonds, and amino and oxygen groups, for instance, can form complexes with Cr(VI) ions, increasing the electrostatic attraction with tea residues [57, 62, 63].

Additionally, pH will have a significant impact on adsorption behavior. The ion speciation of Cr(VI) and the surface charge of the adsorbents are both impacted by the pH of the solution. The experiment's findings showed that at pH 2, when the majority of the adsorbent's functional groups were protonated and became more positively charged, there was the greatest amount of adsorption. Furthermore, in the aqueous phase, Cr(VI) can take on a number of anionic forms, such as chromate (CrO_4^{2-}), dichromate ($Cr_2O_7^{2-}$), and hydrogen chromate ($HCrO_4^-$) (Figure 11) [64, 65]. Within the experimental pH range (below pH_{zpc}), the solution was dominated by negatively charged $Cr_2O_7^{2-}$, $HCrO_4^-$ ions, which were more readily attached to the positively charged functional groups (-OH, -COOH) on the biosorbent due to electrostatic affinity [17, 19, 49].

However, when the pH increased above the pH_{zpc} of the adsorbent, surface protonation declined, the competition between the chromate and OH species became stronger, and the electrostatic attraction between the Cr(VI) species and the surface of the adsorbent decreased, demonstrating a reduction in Cr(VI) removal efficiency and adsorption capability. Furthermore, a low pH promotes the reduction of Cr(VI) ions to Cr(III) ions via the acidic and phenolic groups in the tea residues [66, 67].

According to SEM and BET results, NaOH treatments increased specific surface area in comparison to untreated

Table 9: Comparison of adsorption capacities of tea residues with other adsorbents for Cr(VI) adsorption.

No.	Adsorbents	Optimized conditions	The maximum adsorption capacity ($mg\,g^{-1}$)	References
1	Green tea waste	pH of 2, contact time of 60 minutes, and initial Cr(VI) concentration of $100\,mg\,L^{-1}$	33.9	[17]
2	Tea waste	pH of 3.9, adsorbent dosage of $6\,g\,L^{-1}$, contact time of 240 minutes, and temperature of 303 K	23.3-73.3	[41]
3	Bleached-tea waste	pH of 2, adsorbent dosage of $2.5\,g\,L^{-1}$, contact time of 24 hours, and initial Cr(VI) concentration of 100 ppm	80	[42]
4	Black tea waste	pH of 10 and adsorbent dose of $14\,g\,L^{-1}$	10.64	[48]
5	Mixed tea waste	pH of 2, adsorbent dose of $2\,g\,L^{-1}$, contact time of 180 minutes, temperature of 303-323 K, initial Cr(VI) concentration of 10-30 $mg\,L^{-1}$, and agitation speed of 250 rpm	94.34	[49]
6	Spent tea leaves	pH of 10, adsorbent dose of $2\,g\,L^{-1}$, contact time of 60 minutes, and initial Cr(VI) concentration of $25.6\,mg\,L^{-1}$	3.168	[68]
7	Spent tea leaves	pH of 3, initial Cr(VI) concentration of $50\,mg\,L^{-1}$, adsorbent dose of 0.7625 g, and contact time of 100 min	47.98	[69]
8	Tea waste	Contact time of 60 minutes, room temperature, initial Cr(VI) concentration of 152 ppm, and agitation speed of 100 rpm	5.20	[70]
9	Nanoceria-loaded tea waste	pH of 3, adsorbent dose of 0.8 g, temperature of 333 K, and initial Cr(VI) concentration of $10\,mg\,L^{-1}$	32.15	[71]
10	Red and black tea waste	pH of 2, temperature of 298 K, contact time of 60 minutes	1.4-3.3	[72]
11	Green tea residue Pu-erh residue Tieguanyin residue	pH of 2, adsorbent dose of $2\,g\,L^{-1}$, contact time of 40 minutes for pu-erh, 180 minutes for tieguanyin, and 360 minutes for green tea	6.15 19.50 12.31	Present study

tea residues. Generally, the relationship between increased surface area and enhanced metal uptake was shown to be positive. Increased surface area improved the adsorptive nature of tea residues or increased the number of active binding sites.

Based on the kinetic and isotherm analysis, it was hypothesized that for green tea, adsorption was mostly the result of physical interactions, while for pu-erh and tieguanyin, adsorption was a combination of both physisorption and chemisorption. The main mechanisms controlling the adsorption of Cr(VI) by tea residues were complexation, hydrogen bonding, electrostatic attraction, and reduction reactions.

3.12. Comparisons with Other Different Tea Residue Adsorbents. A comparison of the adsorption characteristics of other tea residues for Cr(V) is presented in Table 9. As can be observed in Table 9, different varieties of tea residues have been found to be effective according to their remarkable adsorption capabilities. The adsorption mechanisms mainly included reduction reactions, complexation, coprecipitation, and ion exchange. It can also be noticed that the three types of tea residues have comparable adsorption capabilities to other adsorbents, implying that they have the potential to remove Cr(V) from aqueous solutions as low-cost adsorbents. Nevertheless, as a result of the differences in structure, composition, and modification methods, the adsorption capacity and mechanism might be different for the adsorption of chromium and other contaminants by different types of tea residues, which needs to be further studied in order to achieve the aim of residue control by residue.

4. Conclusion

In this paper, the adsorption of Cr(VI) from the aqueous solution was completed by using three types of tea residues (green tea, pu-erh, and tieguanyin). Characterization analysis (pH_{zpc}, cellulose content, SEM, BET, XRD, and FTIR) showed that the alkaline treatment, which was inexpensive and environmentally friendly, was a very efficient step to remove hemicellulose, lignin, wax, and pectin from the tea residues. Kinetic studies revealed that all biosorbents followed the pseudo-second model for Cr(VI) adsorption, with pu-erh having the highest rate constant in all three cases. The equilibrium data fit well with the Freundlich isotherm model. The maximum Cr(VI) adsorption capacities of green tea, pu-erh, and tieguanyin residues were found to be 6.15, 19.50, and 12.31 $mg\,g^{-1}$, respectively. Thermodynamic parameters were predicted and indicated that the adsorption was spontaneous and endothermic. Based on this research, the three types of tea residues can serve as appealing adsorbents for the adsorption of wastewater containing Cr(V) ions.

Data Availability

Data are available on request.

Conflicts of Interest

The authors declare that they have no conflicts of interest.

Acknowledgments

The authors would like to thank the Hubei Key Laboratory of Purification and Application of Plant Anti-Cancer Active Ingredients for the financial support. This study was supported by the Scientific Research Project of Hubei Provincial Department of Education (Grant No. D20223001).

References

[1] P. Sharma, S. P. Singh, S. K. Parakh, and Y. W. Tong, "Health hazards of hexavalent chromium (Cr (VI)) and its microbial reduction," *Bioengineered*, vol. 13, no. 3, pp. 4923–4938, 2022.

[2] M. Balali-Mood, K. Naseri, Z. Tahergorabi, M. R. Khazdair, and M. Sadeghi, "Toxic mechanisms of five heavy metals: mercury, lead, chromium, cadmium, and arsenic," *Frontiers in Pharmacology*, vol. 12, p. 643972, 2021.

[3] S. Prasad, K. K. Yadav, S. Kumar et al., "Chromium contamination and effect on environmental health and its remediation: a sustainable approaches," *Journal of Environmental Management*, vol. 285, article 112174, 2021.

[4] U. Chadha, S. K. Selvaraj, S. Vishak Thanu et al., "A review of the function of using carbon nanomaterials in membrane filtration for contaminant removal from wastewater," *Materials Research Express*, vol. 9, article 012003, 2022.

[5] A. Nnam, A. Ahj, B. Ki, A. Rr, and C. Zaa, "Fly ash modified magnetic chitosan-polyvinyl alcohol blend for reactive orange 16 dye removal: adsorption parametric optimization," *International Journal of Biological Macromolecules*, vol. 189, pp. 464–476, 2021.

[6] M. Nur-E-Alam, M. A. Mia, F. Ahmad, and M. M. Rahman, "An overview of chromium removal techniques from tannery effluent," *Applied Water Science*, vol. 10, no. 9, p. 10, 2020.

[7] Y. Shu, B. Ji, B. Cui et al., "Almond shell-derived, biochar-supported, nano-zero-valent iron composite for aqueous hexavalent chromium removal: performance and mechanisms," *Nanomaterials*, vol. 10, no. 2, p. 198, 2020.

[8] S. U. Din, M. S. Khan, S. Hussain et al., "Adsorptive mechanism of chromium adsorption on siltstone-nanomagnetite-biochar composite," *Journal of Inorganic and Organometallic Polymers and Materials*, vol. 31, no. 4, pp. 1608–1620, 2021.

[9] H. Dong, H. Liang, L. Yang et al., "Porous biochar derived from waste distiller's grains for hexavalent chromium removal: adsorption performance and mechanism," *Journal of Environmental Chemical Engineering*, vol. 11, no. 3, p. 110137, 2023.

[10] U. Jamil, M. Zeeshan, S. R. Khan, and S. Saeed, "Synthesis and two-step KOH based activation of porous biochar of wheat straw and waste tire for adsorptive exclusion of chromium (VI) from aqueous solution; thermodynamic and regeneration study," *Journal of Water Process Engineering*, vol. 53, p. 103892, 2023.

[11] A. Hariharan, V. Harini, S. Sandhya, and S. Rangabhashiyam, "Waste Musa acuminata residue as a potential biosorbent for the removal of hexavalent chromium from synthetic wastewater," *Biomass Conversion and Biorefinery*, vol. 13, pp. 1297–1310, 2023.

[12] M. A. Hashem, M. A. Momen, M. Hasan, M. S. Nur-A-Tomal, and M. H. Sheikh, "Chromium removal from tannery wastewater using Syzygium cumini bark adsorbent," *International journal of Environmental Science and Technology*, vol. 16, no. 3, pp. 1395–1404, 2019.

[13] T. S. Badessa, E. Wakuma, and A. Yimer, "Bio-sorption for effective removal of chromium(VI) from wastewater using Moringa stenopetala seed powder (MSSP) and banana peel powder (BPP)," *BMC Chemistry*, vol. 14, no. 1, p. 71, 2020.

[14] L. D. Senanu, G. Kranjac-Berisavljevic, and S. J. Cobbina, "The use of local materials to remove heavy metals for household-scale drinking water treatment: a review," *Environmental Technology and Innovation*, vol. 29, p. 103005, 2023.

[15] D. L. Huang, B. Li, J. G. Ou et al., "Megamerger of biosorbents and catalytic technologies for the removal of heavy metals from wastewater: preparation, final disposal, mechanism and influencing factors," *Journal of Environmental Management*, vol. 261, p. 109879, 2020.

[16] B. S. Inbaraj, K. Sridhar, and B. H. Chen, "Removal of polycyclic aromatic hydrocarbons from water by magnetic activated carbon nanocomposite from green tea waste," *Journal of Hazardous Materials*, vol. 415, p. 125701, 2021.

[17] C. Timbó, M. Kandawa-Schulz, M. O. Amuanyena, and H. M. Kwaambwa, "Adsorptive removal from aqueous solution of Cr(VI) by green moringa tea leaves biomass," *Journal of Encapsulation and Adsorption Sciences*, vol. 7, no. 2, pp. 108–119, 2017.

[18] V. T. Le, M. U. Dao, H. S. Le, D. L. Tran, V. D. Doan, and H. T. Nguyen, "Adsorption of Ni(II) ions by magnetic activated carbon/chitosan beads prepared from spent coffee grounds, shrimp shells and green tea extract," *Environmental Technology*, vol. 41, no. 21, pp. 2817–2832, 2020.

[19] P. S. Katha, Z. Ahmed, R. Alam, B. Saha, and M. S. Rahman, "Efficiency analysis of eggshell and tea waste as low cost adsorbents for Cr removal from wastewater sample," *South African Journal of Chemical Engineering*, vol. 37, pp. 186–195, 2021.

[20] S. T. Kadhum, G. Y. Alkindi, and T. M. Albayati, "Eco friendly adsorbents for removal of phenol from aqueous solution employing nanoparticle zero-valent iron synthesized from modified green tea bio-waste and supported on silty clay," *Chinese Journal of Chemical Engineering*, vol. 36, no. 8, pp. 19–28, 2021.

[21] H. Çelebi, G. Gök, and O. Gök, "Adsorption capability of brewed tea waste in waters containing toxic lead(II), cadmium (II), nickel (II), and zinc(II) heavy metal ions," *Scientific Reports*, vol. 10, no. 1, p. 17570, 2020.

[22] H. Cai, H. Zou, J. Liu et al., "Thermal degradations and processes of waste tea and tea leaves via TG-FTIR: combustion performances, kinetics, thermodynamics, products and optimization," *Bioresource Technology*, vol. 268, pp. 715–725, 2018.

[23] K. Wang, X. Tang, L. Liu et al., "Adsorption of Cr (VI) from water by modified tea residue biochar," *Shangdong Chemical Industry*, vol. 51, no. 21, pp. 5–10, 2022.

[24] C. Valerio Cárdenas, J. Martínez-Herrera, D. L. Velázquez-Vargas, and P. De la Cruz-Burelo, "Determination of the point of zero charge of pineapple (Ananas comosus L.) peel and its application as copper adsorbent," *Agro Productividad*, vol. 14, pp. 53–59, 2021.

[25] X. Liu, J. F. Wen, Y. R. Jiao, and Y. L. Wang, "Determination of cellulose, hemicellulose and lignin content in abandoned fruit core shell," *Journal of Yulin University*, vol. 32, no. 2, pp. 6–9, 2022.

[26] J. T. Carvalho, P. A. Milani, J. L. Consonni, G. Labuto, and E. N. Carrilho, "Nanomodified sugarcane bagasse biosorbent: synthesis, characterization, and application for Cu(II) removal from aqueous medium," *Environmental Science and Pollution Research*, vol. 28, pp. 24744–24755, 2020.

[27] A. Anjum, S. A. Mazari, Z. Hashmi et al., "A review of novel green adsorbents as a sustainable alternative for the remediation of chromium (VI) from water environments," *Heliyon*, vol. 9, no. 5, article e15575, 2023.

[28] A. A. Azzaz, S. Jellali, H. Akrout, A. A. Assadi, and L. Bousselmi, "Optimization of a cationic dye removal by a chemically modified agriculture by-product using response surface methodology: biomasses characterization and adsorption properties," *Environmental Science and Pollution Research*, vol. 24, no. 11, pp. 9831–9846, 2017.

[29] J. Zhao and Y. Dai, "Tetracycline adsorption mechanisms by NaOH-modified biochar derived from waste Auricularia auricula dregs," *Environmental Science and Pollution Research*, vol. 29, no. 6, pp. 9142–9152, 2022.

[30] P. Patel, S. Gupta, and P. Mondal, *Modeling and optimization of process parameters of MB dye adsorption using waste-derived chemically activated biosorbents*, Biomass Conversion and Biorefinery, 2022.

[31] Ş. Taşar and A. Özer, "A comparative study of hemicellulose isolation with hot water, alkaline, and delignification methods from tea leaf brewing waste," *Biomass Conversion and Biorefinery*, vol. 12, no. 7, pp. 2501–2514, 2022.

[32] C. Indolean, S. Burcă, and A. Măicăneanu, "Adsorptive removal of malachite green from model aqueous solutions by chemically modified waste green tea biomass," *Acta Chimica Slovenica*, vol. 64, no. 2, pp. 513–521, 2017.

[33] J. Wen, Y. Yin, X. Peng, and S. Zhang, "Using H_2O_2 to selectively oxidize recyclable cellulose yarn with high carboxyl content," *Cellulose*, vol. 26, no. 4, pp. 2699–2713, 2019.

[34] D. N. Barman, M. A. Haque, M. M. Hossain, S. K. Paul, and H. D. Yun, "Deconstruction of pine wood (Pinus sylvestris) recalcitrant structure using alkali treatment for enhancing enzymatic saccharification evaluated by Congo red," *Waste and Biomass Valorization*, vol. 11, pp. 1–10, 2020.

[35] N. A. Salahuddin, M. A. Abdelwahab, A. M. Akelah, and M. Elnagar, "Adsorption of Congo red and crystal violet dyes onto cellulose extracted from Egyptian water hyacinth," *Natural Hazards*, vol. 105, no. 2, pp. 1375–1394, 2021.

[36] E. Allanas, A. M. Rahman, E. M. Arlin, and E. A. Prasetyanto, "Study surface area and pore size distribution on synthetic zeolite X using BET, BJH and DFT methods," *Journal of Physics: Conference Series*, vol. 2019, article 012094, 2021.

[37] P. Boonsuk, A. Sukolrat, S. Bourkaew et al., "Structure-properties relationships in alkaline treated rice husk reinforced thermoplastic cassava starch biocomposites," *International Journal of Biological Macromolecules*, vol. 167, pp. 130–140, 2020.

[38] A. Ateş, "Effect of alkali-treatment on the characteristics of natural zeolites with different compositions," *Journal of Colloid and Interface Science*, vol. 523, pp. 266–281, 2018.

[39] F. Njeh, M. Hamza, I. Bouaziz, R. Abdelhédi, and M. Abdelmouleh, "Isolation, characterization and methylene blue adsorption: application of cellulose from olive sawdust," *Korean Journal of Chemical Engineering*, vol. 39, no. 3, pp. 760–774, 2022.

[40] H. S. Kassa, S. A. Jabasingh, S. A. Mohammed, S. Baek, and S. Park, "Extraction and characterization of cellulose nanocrystals from anchote (Coccinia abyssinica) bagasse," *Macromolecular Research*, vol. 30, no. 11, pp. 776–782, 2022.

[41] M. Nigam, S. Rajoriya, S. R. Singh, and P. Kumar, "Adsorption of Cr (VI) ion from tannery wastewater on tea waste: kinetics, equilibrium and thermodynamics studies," *Journal of Environmental Chemical Engineering*, vol. 7, no. 3, article 103188, 2019.

[42] J. Wu, H. Annath, H. Chen, and C. Mangwandi, "Upcycling tea waste particles into magnetic adsorbent materials for removal of Cr(VI) from aqueous solutions," *Particuology*, vol. 80, pp. 115–126, 2023.

[43] A. Bondarev, D. Popovici, C. Călin, S. Mihai, E. Sîrbu, and R. Doukeh, "Black tea waste as green adsorbent for nitrate removal from aqueous solutions," *Materials*, vol. 16, no. 12, p. 4285, 2023.

[44] A. Karn, S. J. Thakur, and B. Shrestha, "Extraction and characterization of cellulose from agricultural residues: wheat straw and sugarcane bagasse," *Journal of Nepal Chemical Society*, vol. 43, no. 1, pp. 93–98, 2022.

[45] Y. Alvarez-Galvan, B. Minofar, Z. Futera et al., "Adsorption of hexavalent chromium using activated carbon produced from Sargassum ssp.: comparison between lab experiments and molecular dynamics simulations," *Molecules*, vol. 27, no. 18, article 6040, 2022.

[46] H. J. Abdoul, M. H. Yi, M. Prieto et al., "Efficient adsorption of bulky reactive dyes from water using sustainably-derived mesoporous carbons," *Environmental Research*, vol. 221, article 115254, 2023.

[47] A. Ajmani, T. Shahnaz, S. Narayanan, and S. Narayanasamy, "Equilibrium, kinetics and thermodynamics of hexavalent chromium biosorption on pristine and zinc chloride activated Senna siamea seed pods," *Chemistry and Ecology*, vol. 35, no. 4, pp. 379–396, 2019.

[48] M. Nur-E-Alam, M. Abu Sayid Mia, F. Ahmad, and M. Mafizur Rahman, "Adsorption of chromium (Cr) from tannery wastewater using low-cost spent tea leaves adsorbent," *Applied Water Science*, vol. 8, no. 5, pp. 1–7, 2018.

[49] W. Cherdchoo, S. Nithettham, and J. Charoenpanich, "Removal of Cr(VI) from synthetic wastewater by adsorption onto coffee ground and mixed waste tea," *Chemosphere*, vol. 221, pp. 758–767, 2019.

[50] X. Zhang, S. Wu, Y. Liu, Z. Wang, H. Zhang, and R. Xiao, "Removal of Cr(VI) from aqueous solution by rice-husk-based activated carbon prepared by dual-mode heating method," *Carbon Resources Conversion*, vol. 6, no. 2, pp. 76–84, 2023.

[51] A. Yilmaz Camoglu, D. Ozdes, and C. Duran, "Adsorption behaviour of EDTA modified magnetic Fe_3O_4 coated brewed tea waste on Cr(VI) removal," *Chemistry Africa*, vol. 6, no. 2, pp. 921–931, 2023.

[52] M. Abdel Salam, M. R. Abukhadra, and A. Adlii, "Insight into the adsorption and photocatalytic behaviors of an organo-bentonite/Co_3O_4 green nanocomposite for malachite green synthetic dye and Cr(VI) metal ions: application and mechanisms," *ACS Omega*, vol. 5, no. 6, pp. 2766–2778, 2020.

[53] Z. Tattibayeva, S. Tazhibayeva, W. Kujawski, B. Zayadan, and K. Musabekov, "Peculiarities of adsorption of Cr (VI) ions on the surface of Chlorella vulgaris ZBS1 algae cells," *Heliyon*, vol. 8, no. 9, article e10468, 2022.

[54] M. I. Jalees, M. U. Farooq, S. Basheer, and S. Asghar, "Removal of heavy metals from drinking water using Chikni Mitti (kaolinite): isotherm and kinetics," *Arabian Journal for Science and Engineering*, vol. 44, no. 7, pp. 6351–6359, 2019.

[55] U. Khalil, M. Bilal Shakoor, S. Ali, M. Rizwan, M. Nasser Alyemeni, and L. Wijaya, "Adsorption-reduction performance of tea waste and rice husk biochars for Cr(VI) elimination from wastewater," *Journal of Saudi Chemical Society*, vol. 24, no. 11, pp. 799–810, 2020.

[56] A. Villabona Ortíz, C. N. Tejada-Tovar, and R. Ortega Toro, "Adsorption thermodynamics of Cr(VI) removal by using agro-industrial waste of oil palm bagasse and plantain peels," *Revista Ingenieria E Investigacion*, vol. 40, no. 3, pp. 22–28, 2020.

[57] Y. A. Neolaka, Y. Lawa, J. N. Naat et al., "The adsorption of Cr(VI) from water samples using graphene oxide-magnetic (GO-Fe_3O_4) synthesized from natural cellulose-based graphite (kusambi wood or Schleichera oleosa): study of kinetics, isotherms and thermodynamics," *Journal of Materials Research and Technology*, vol. 9, no. 3, pp. 6544–6556, 2020.

[58] Z. Saigl and S. Al-Dafeeri, "Selective separation of chromium (VI) from aqueous solutions by adsorption onto truffle peels as novel biomass," *International Journal of Environmental Analytical Chemistry*, vol. 103, pp. 928–946, 2021.

[59] E. A. Abdel-Galil, L. M. Hussin, and W. M. El-kenany, "Adsorption of Cr(VI) from aqueous solutions onto activated pomegranate peel waste," *Desalination and Water Treatment*, vol. 211, pp. 250–266, 2021.

[60] E. Altintiga, M. Karakasb, N. Basokb, and H. Altundagc, "Adsorption behaviour of Cr(VI) on activated carbon: isotherm, kinetic, and thermodynamic studies," *Desalination and Water Treatment*, vol. 217, pp. 221–231, 2021.

[61] T. Naseem, F. Bibi, S. Arif et al., "Adsorption and kinetics studies of Cr (VI) by graphene oxide and reduced graphene oxide-zinc oxide nanocomposite," *Molecules*, vol. 27, no. 21, p. 7152, 2022.

[62] M. A. Campagnolo, A. C. Celso Gonçalves, D. Schwantes, D. Dragunski, T. Demetrio, and L. H. Deminski, "Cr(total) removal using chicken feathers derived materials: a laboratory study with adsorption-precipitation in electroplating effluents," *Separation Science and Technology*, vol. 57, no. 12, pp. 1910–1925, 2022.

[63] Z. Li, C. Yang, G. Qu et al., "Chitosan-modified magnetic carbon nanomaterials with high efficiency, controlled motility, and reusability-for removal of chromium ions from real wastewater," *Environmental Science and Pollution Research*, vol. 30, no. 17, pp. 51271–51287, 2023.

[64] B. A. Marinho, R. O. Cristóvão, R. A. Boaventura, and V. J. Vilar, "As(III) and Cr(VI) oxyanion removal from water by advanced oxidation/reduction processes-a review," *Environmental Science and Pollution Research*, vol. 26, pp. 2203–2227, 2018.

[65] C. M. Stern, D. W. Hayes, L. O. Kgoadi, and N. Elgrishi, "Emerging investigator series: carbon electrodes are effective for the detection and reduction of hexavalent chromium in water," *Environmental Science: Water Research & Technology*, vol. 6, pp. 1256–1261, 2020.

[66] B. Yan and Z. Chen, "Influence of pH on Cr(VI) reduction by organic reducing substances from sugarcane molasses," *Applied Water Science*, vol. 9, no. 3, pp. 1–8, 2019.

[67] Y. Fei, M. Li, Z. Ye et al., "The pH-sensitive sorption governed reduction of Cr(VI) by sludge derived biochar and the

accelerating effect of organic acids," *Journal of Hazardous Materials*, vol. 423, article 127205, 2022.

[68] A. S. Mia, U. Ali, R. M. Nur-E-Alam, and Z. Alam, "Removal of heavy metals from tannery wastewater by using sawdust and spent tea leaves as an adsorbent," *Physical Science & Biophysics Journal*, vol. 4, no. 1, article 000139, 2020.

[69] I. H. Dakhil, "Adsorption of chromium (VI) from aqueous solutions using low cost adsorbent: equilibrium and regeneration studies," *Journal of Engineering*, vol. 19, no. 11, p. 1406, 2023.

[70] M. Mariana and F. Mulana, "Adsorption of heavy metal Cr (VI) using biosorbent of tea dregs: experimental and modeling," *Proceedings of the 5th Annual International Conference Syiah Kuala University in Conjunction with the 8th International Conference of Chemical Engineering on Science and Applications*, pp. 93–99, 2015.

[71] U. K. Sahu, Y. Zhang, W. Huang et al., "Nanoceria-loaded tea waste as bio-sorbent for Cr(VI) removal," *Materials Chemistry and Physics*, vol. 290, p. 126563, 2022.

[72] Z. N. Majeed, S. A. Farhan, R. M. Dadoosh, and H. H. Mohammed, "Using spent tea residue to elimination of chromium in aqueous liquid," *Journal of Physics: Conference Series*, vol. 1664, article 012082, p. 127205, 2020.